# Rat Hepatic Microsomal Aldehyde Dehydrogenase. Identification of 3- and 4-Substituted Aromatic Aldehydes as Substrates of the Enzyme

Robert Martini and Michael Murray*

*Storr Liver Unit, Department of Medicine, University of Sydney, Westmead Hospital, Westmead, New South Wales 2145, Australia*

*Received June 21, 1995*[⊗]

The rat hepatic microsomal aldehyde dehydrogenase (mALDH) metabolizes aliphatic and aromatic aldehydes to the corresponding acids with NAD as the optimal cofactor. However, dehydrogenation of the aliphatic compounds is substantially more efficient. In the present study, a series of aromatic aldehydes was evaluated as substrates of the purified mALDH so that the physicochemical factors that contribute to substrate affinity could be evaluated. Substitution of the aromatic system in the 3- and 4-positions produced relatively good substrates, but 2-substituted congeners did not undergo dehydrogenation. However, aldehydes with hydrophilic substituents in the 3- or 4-positions and those with extremely bulky substituents at both positions (e.g., 3,4-dibenzyloxy) were also poor substrates for the enzyme and dehydrogenation was undetectable. A quantitative structure−activity relationship was determined that related the logarithm of the Michaelis constants for 27 substituted aromatic aldehydes with the zero-order connectivity function of the molecule ($^0\chi$), the shapes of the 3- and 4-substituents ($\kappa$), and the electronic nature of the 4-substituent ($\sigma$). In this equation, 81% of the data variance was explained. From a consideration of the dimensions of 3-phenoxybenzaldehyde, which was a relatively good substrate, the mALDH possesses a narrow cleft within the active site that is at least 7.5 Å wide and extends at least 12 Å from the the catalytic residue (probably cysteine). Previously established relationships between connectivity functions and molecular polarizability suggest that dipolar interactions within the active site, as well as dispersion forces, may play a role in substrate specificity. Although optimal shapes for carbocyclic substituents were not provided by the analysis, the unfavorable effect on dehydrogenation from hydrophilic and large substituents suggests that the active site of the mALDH is relatively rigid and that the orientation of the substrate in relation to the catalytic cysteine and the cofactor binding site is critical.

## Introduction

Aldehydes are present in the diet and the environment and are also formed in many biological reactions, including the oxidative deamination of neurotransmitters and the peroxidation of lipids during xenobiotic monooxygenation (*1*). Aldehyde dehydrogenase (ALDH)[1] enzymes are important in the detoxification of aldehydes and catalyze their conversion to the corresponding carboxylic acids. ALDHs are widely distributed in most mammalian tissues, and it is now clear that there are multiple forms of these enzymes. Mammalian liver contains a number of ALDHs; several have been isolated from the cytosolic, mitochondrial, and microsomal (endoplasmic reticulum) fractions (*2*−*4*). ALDHs have been grouped into several classes on the basis of cDNA sequence alignment; a number of substrate-specific ALDHs have not yet been assigned to classes (*5*). Class 3 ALDHs constitute a diverse group, including the constitutive microsomal form (mALDH), the constitutive cytosolic corneal form, and a 2,3,7,8-tetrachlorodibenzo-*p*-dioxin (TCDD)-inducible cytosolic form that is also expressed in tumor cells (*6*−*10*).

Many aldehydes are dehydrogenated by ALDHs, and attempts have been made to rationalize the substrate specificity of the enzymes on the basis of subcellular location. Although generalization is difficult, mitochondrial and cytosolic forms of ALDH (principally classes 1 and 2) are more efficient catalysts in the NAD-supported dehydrogenation of acetaldehyde and propionaldehyde (*1*). The TCDD-inducible class 3 ALDH preferentially catalyzes the NADP-mediated oxidation of benzaldehyde, and the mALDH readily accommodates medium- to long-chain aliphatic aldehydes and uses NAD as the cofactor (*1*).

Interest in the mALDH has developed with its possible role in the detoxification of products of lipid peroxidation, including hexanal and hydroxynonenal (*11*−*13*). In view of the hydrophobic nature of the microsomal environment, it is perhaps not surprising that the mALDH is an efficient catalyst in the dehydrogenation of long-chain aldehydes. However, benzaldehyde, an aromatic aldehyde of a hydrophobicity similar to pentanal (log $P_{\text{octanol/water}}$ values of 1.48 and 1.54, respectively), is a poor substrate for the enzyme. Thus, lipophilicity does not appear to be the sole factor that determines the substrate specificity of the mALDH. It has been suggested that halo-substituted aromatic aldehydes may be better substrates than benzaldehyde for the mALDH (*14*). The present study investigated the role of the mALDH in the dehydrogenation of a series of substituted aromatic aldehydes. A quantitative structure−activity relationship (QSAR) was derived that accounted for 81% of the data variance

[⊗] Abstract published in *Advance ACS Abstracts,* December 15, 1995.

[1] Abbreviations: ALDH, aldehyde dehydrogenase; IgG, immunoglobulin G; mALDH, microsomal aldehyde dehydrogenase; QSAR, quantitative structure−activity relationship; TCDD, 2,3,7,8-tetrachlorodibenzo-*p*-dioxin.

0893-228x/96/2709-0268$12.00/0 

in terms of the molecular connectivity of the substrate and the shape and electronic nature of the substituents.

## Materials and Methods

**Chemicals.** Aldehydes used in this study were the highest grade commercially available and were obtained from either Sigma Chemical Co. (St Louis, MO) or Aldrich Chemicals (Milwaukee, WI). NAD and detergents were also purchased from Sigma. DE-52-cellulose was purchased from Whatman (Kent, England), 5′-AMP-Sepharose 4B was obtained from Pharmacia (Uppsala, Sweden), and hydroxylapatite (BioGel HT) and DEAE Affigel Blue were purchased from Bio-Rad (Richmond, CA). Extracti-Gel D was from Pierce Chemicals (Rockford, IL).

**Synthesis of Isomeric (Chlorophenyl)acetaldehydes.** The synthesis of (4-chlorophenyl)acetaldehyde (*31*) is described. (4-Chlorophenyl)ethanol (10 g) was added slowly to an ice-cold solution of saturated $K_2Cr_2O_7$ (25 mL) and concentrated $H_2SO_4$ (5 mL). The solution turned green almost immediately and was diluted with 250 mL of distilled water after 20 min. Solid $NaHCO_3$ was added and, after the evolution of $CO_2$ had ceased, the solution was transferred to a separatory funnel and diethyl ether (250 mL) was added. After extraction, the lower (aqueous) layer was discarded and the ether layer was washed twice with 250 mL portions of distilled water. Anhydrous $Na_2SO_4$ was added; the ether was decanted and removed under a stream of $N_2$. From the resultant oil the desired compound (*31*) was obtained by distillation (bp 160−161 °C; lit. bp 114−116 °C (13 mmHg) (*15*)). No attempt was made to optimize the yield, which was ∼10%.

**Animals.** Microsomes were prepared from homogenized livers of adult male rats by differential ultracentrifugation (*16*), with an additional wash step to minimize contamination of microsomes with cytosolic protein. Microsomal protein concentrations were determined by the method of Lowry *et al.* (*17*).

**Assay of ALDH Activity.** ALDH activity was assayed spectrophotometrically at 340 nm, which monitors the formation of NADH from NAD (*18*). Incubations were routinely performed in 0.1 M phosphate buffer (pH 7.4) that contained EDTA (1 mM), Triton X-100 (0.009%), and NAD (1 mM). Aldehydes (usually 1 mM, except in the determination of kinetic parameters) were introduced into incubations in dimethylformamide (10 μL); this volume of solvent did not influence reaction rate. Triton X-100 was required for dissolution of some of the more highly substituted aromatic aldehydes; the concentration of detergent employed did not influence rates of microsomal decanal dehydrogenation. The reaction was performed at 37 °C and was initiated by addition of purified enzyme (0.5−2 μg). ALDH activity was not detected in the absence of cofactor, substrate, or protein. In immunoinhibition experiments, the microsomal protein (40 μg) and anti-mALDH immunoglobulin G (IgG) were preincubated together for 30 min at 37 °C; cofactor was then used to initiate the reaction.

**Isolation of the mALDH from Rat Liver**. The mALDH was purified from 0.5% cholate-solubilized hepatic fractions in a fashion similar to previously published procedures (*2, 11, 18*). A single protein, with apparent molecular mass of 54 kDa as determined by SDS−polyacrylamide gel electrophoresis, was obtained following chromatography on DEAE-cellulose, 5′-AMP-Sepharose 4B, and hydroxylapatite.

Typically, microsomes (∼1000 mg) were treated with sodium cholate (to a final concentration of 0.5%) for 1 h, centrifuged at 105000*g* for 1 h, and applied to a column of Whatman DE-52 (2.5 × 20 cm) that had been equilibrated with buffer A (10 mM potassium phosphate buffer (pH 7.4) containing 20% glycerol, EDTA (100 μM), dithioerythritol (100 μM), 0.5% cholate, and 0.1% Lubrol PX) at a flow rate of 60 mL/h. After loading, the column was washed with buffer A, followed by a NaCl gradient. Protein elution was monitored at 280 nm, and ALDH activity was determined with decanal (1 mM) and NAD (1 mM). Decanal dehydrogenation activity was eluted in the unbound fractions, which were pooled and loaded onto 5′-AMP-Sepharose 4B.

The 5′-AMP-Sepharose 4B column (1.5 × 10 cm) was equilibrated with buffer A. After loading of the sample, the column was washed with buffer A, followed by 50 mM potassium phosphate buffer, pH 7.4 (flow rate 60 mL/h), and finally, with buffer A containing 0.5 mM NAD. Although most of the protein did not bind to this column, the major portion of the decanal dehydrogenation activity was eluted with NAD.

Fractions containing enzyme activity were diluted to 10 mM potassium phosphate (pH 7.4) and applied to a hydroxylapatite column (1 × 4 cm) that had been equilibrated with buffer A. The mALDH bound to this column and was eluted with 50 mM potassium phosphate (pH 7.4) that contained 20% glycerol, 0.1% Lubrol PX, 0.5% cholate, and EDTA (100 μM). The final preparation appeared homogeneous after electrophoresis on 7.5% SDS−polyacrylamide gels (*19*). Decanal dehydrogenation activity catalyzed by the preparation was enriched 25-fold, and 17% of the activity present in cholate-solubilized microsomes was recovered. The detergents were removed from the active fractions on ExtractiGel D.

**Preparation of the Anti-mALDH IgG.** Small quantities of the purified mALDH (200 μg) were injected subcutaneously into female New Zealand white rabbits in a 1:1 mixture with Freund's complete adjuvant. Two further injections were performed at 2 week intervals with mALDH in Freund's incomplete adjuvant. Ten days after the third inoculation, blood was taken from the ear vein, clotted, and centrifuged to yield the serum. The IgG was precipitated with ammonium sulfate (40%), and the resultant pellet was resuspended in buffer B (0.02 M Tris-HCl buffer (pH 8.0) containing 0.028 M NaCl and 0.02% $NaN_3$) for extensive dialysis against buffer B. The dialysate was applied to a DEAE Affigel Blue column (2.5 × 10 cm) previously equilibrated with buffer B, and the IgG fraction passed through the column in the unbound fraction.

**Derivation of Physicochemical Parameters Used in Regression Analysis.** Hydrophobic (log *P* and $\pi$), electronic ($\sigma$), and steric (MR; molar refractivity) constants were taken from the literature (*20, 21*) or calculated according to the additivity principle. MR values were scaled by 0.1 to yield more manageable coefficients.

Molecular connectivity indexes ($^m\chi^t$) were calculated by the methods of Kier and Hall (*22*). In this expression, *m* refers to the order of the connectivity function (the number of bonds over which the calculation was performed, i.e., 0−4) and *t* refers to the arrangement of bonds within the calculated connectivity function (path, cluster, or path/cluster). Valence deltas ($\delta^v$) were obtained from the literature (*23*). For example the first-order molecular connectivity expression is calculated as

$$^1\chi = \sum_{z=1}^{n} (\delta_i^{\,v}\delta_j^{\,v})_z^{\,-0.5}$$

where *n* is the number of component subgraphs (or single-bond path lengths) in the structure and *i* and *j* correspond to the atoms of the subgraph. Higher order $\chi$ indexes were determined similarly, and $\chi$ indexes for 3- and 4-substituents of benzaldehyde derivatives were calculated so that atoms belonging to the basic aromatic nucleus were excluded.

Molecular shape indexes ($^m\kappa_\alpha$) were calculated according to the principles outlined by Kier (*24*). Again, *m* refers to the order of the function (the number of bonds giving rise to the particular subgraph) and α indicates that modified atom counts were used (to adequately describe non-$sp^3$-hybridized atoms and heteroatoms in the analysis). $\kappa$ indexes were used to calculate Ξ, a parameter derived from molecular graphs that describes substituent steric effects and that is calculated from the expression $2^1\kappa_\alpha - {}^0\kappa_\alpha - {}^3\kappa_\alpha$ (*24*). Shape descriptors for 3- or 4-substituents of benzaldehyde derivatives were calculated according to the procedure outlined by Kier (*25*). In this method, the substituent is treated as a dimer, the shape descriptor is then calculated, and the value is halved; this is necessary to adequately describe the shapes of small substituents using the molecular graph approach.

**Table 1. Purification of the mALDH from Rat Liver[a]**

| | specific activity (nmol (mg of protein)$^{-1}$) | total activity ($\mu$mol) | recovery (% of activity) | fold purifn |
|---|---|---|---|---|
| solubilized microsomes | 230 ± 32 | 228.6 ± 31.9 | 100 | 1 |
| DEAE-cellulose | 348 ± 42 | 185.0 ± 26.5 | 81 | 1.5 |
| 5′-AMP-Sepharose 4B | 4750 ± 460 | 93.9 ± 3.7 | 41 | 20.7 |
| hydroxylapatite | 5760 ± 620 | 38.7 ± 3.0 | 17 | 25 |

[a] Data are expressed as mean ± SEM for three separate purification procedures.

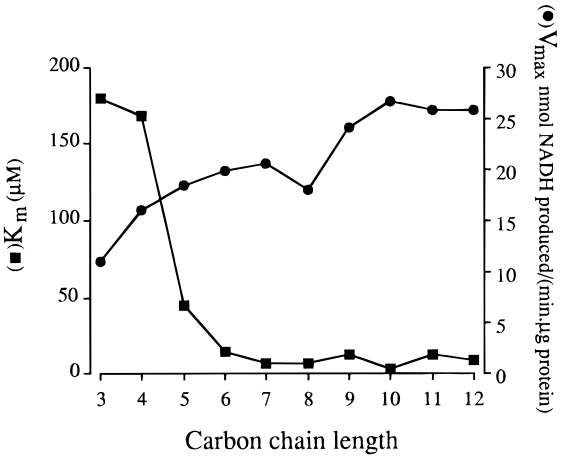


**Figure 1.** Dehydrogenation of aliphatic aldehydes by the purified mALDH. Relationship between alkyl chain length and Michaelis constant ($K_m$) and maximal reaction velocity ($V_{max}$).

From the foregoing, 45 different parameters were derived that described the physicochemical nature of the molecules. Of these, 15 were applied to the analysis of the role of the 3-substituent in aromatic aldehyde dehydrogenation, 15 to the analysis of the role of the 4-substituent, and 15 that described the molecule as a whole or as the sum of the substituents.

**Derivation of Regression Equations and Statistical Analysis.** Regression equations were determined using the STATVIEW program for Macintosh computers. The quality of fit of the data was assessed by determination of the correlation coefficient ($r$), the standard deviation from the regression ($s$), and the $F$ ratio for the analysis. Inclusion of additional parameters into equations was done only where (i) the parameters were not collinear ($r^2$ < 50%; from the correlation matrix performed on each data set), (ii) the second parameter was significant ($t$ test significant at least at the 5% level), and (iii) the $F$ ratio for inclusion of additional parameters was significant. The predictive capacities of eqs 1−10 in Table 5 were assessed by determination of the predictive residual sum of squares (PRESS), variance, or squared correlation coefficient, of predictions ($Q^2$), and standard deviation of predictions ($s_{PRESS}$) values (*26*−28).

Data are presented throughout as mean ± standard error of the mean.

## Results

**Isolation and Characterization of the ALDH from Rat Hepatic Microsomes.** Rat hepatic microsomes catalyze the efficient dehydrogenation of aliphatic aldehydes such as decanal, especially with NAD as cofactor. In this study, the mALDH was purified to homogeneity by column chromatography. The purified protein exhibited a 25-fold greater specific activity in the dehydrogenation of decanal than that present in solubilized microsomes (Table 1). From Figure 1 it is evident that the apparent affinity of the purified enzyme for *n*-alkylaldehydes increased (decrease in $K_m$) with chain length and attained an apparent optimum with decanal ($K_m$ 3.2 $\mu$M). The maximal reaction velocity ($V_{max}$) was also noted with decanal (26.7 nmol of NADH produced min$^{-1}$ ($\mu$g of protein)$^{-1}$), although similar $V_{max}$ values were obtained with nonanal, undecanal, and dodecanal. Several aliphatic aldehydes containing branched alkyl chains were also evaluated as substrates for the mALDH. Branching at the α-carbon decreased the $V_{max}$ for dehydrogenation compared with the corresponding unbranched aldehyde (data not shown). Further methyl substitution at the carbon $\beta$ to the carbonyl group resulted in a decrease in the affinity of the aldehyde for the mALDH.

**Table 2. Effect of *Ortho, Meta,* and *Para* Substitution of Benzaldehyde on the Substrate Dehydrogenation Activity Catalyzed by the mALDH[a]**

| | activity (nmol of NADH produced min$^{-1}$ ($\mu$g of protein)$^{-1}$) | | |
|---|---|---|---|
| substituent | *ortho* | *meta* | *para* |
| chloro | <0.93 | 9.80 | 4.66 |
| cyano | <0.93 | 7.46 | 6.07 |
| methyl | <0.93 | 3.73 | 1.40 |

[a]Data are expressed as the mean of duplicate determinations. Substrate and NAD concentrations were 1mM. The reaction was initiated by the addition of 0.69$\mu$g of purified mALDH.

**Dehydrogenation of Aromatic Aldehydes by the mALDH.** The simplest aromatic aldehyde, benzaldehyde, was a poor substrate for the purified mALDH. An expanded series of substituted aromatic aldehydes was subsequently tested, since it has been suggested that certain analogues may undergo relatively efficient mALDH-mediated dehydrogenation (*14*). The data in Table 2 indicate that substitution of the aromatic ring *ortho* to the carbonyl group resulted in analogues that did not undergo detectable dehydrogenation by the purified mALDH. This was observed when the substituent was chloro, methyl, and cyano and therefore seemed unrelated to the size of the group or whether it was electron releasing or withdrawing. In contrast, the analogous *para*- and, in particular, *meta*-substituted benzaldehydes were quite good substrates for the mALDH. Therefore, 3- and 4-substituted benzaldehydes were selected for further study.

The data in Table 3 indicate that, although the apparent affinity of the mALDH for benzaldehyde was low ($K_m$ 2.9 mM), the maximal reaction velocity was similar to those observed with aliphatic aldehydes ($V_{max}$ 19.4 nmol of NADH produced min$^{-1}$ ($\mu$g of protein)$^{-1}$). In general, as reflected by smaller $K_m$ or larger $V_{max}$ values, the 3-substituted aromatic aldehydes appeared to be superior to their 4-substituted analogues as substrates for the mALDH (Table 3). The smallest $K_m$ value that was determined for an aromatic aldehyde was 85 $\mu$M for 4-phenoxybenzaldehyde (**22**). Other aromatic substrates that were dehydrogenated efficiently by the mALDH were the substituted 3-phenoxybenzaldehydes (**21**, **23**−**25**). These values are similar to those determined for butanal and pentanal but were at least 25-fold greater (lower affinity) than the $K_m$ for decanal, the best substrate for the enzyme. However, in the case of the 3-substituted phenoxybenzaldehydes, $V_{max}$ values were

**Table 3. Kinetic Parameters of the Dehydrogenation of Aromatic Aldehydes by the mALDH[a]**

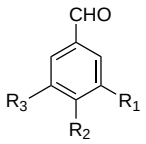


| | aldehyde | $R_1$ | $R_2$ | $R_3$ | $K_m$ ($\mu$M) | $V_{max}$ (nmol min$^{-1}$ ($\mu$g of protein)$^{-1}$) | $10^6 V_{max}/K_m$ |
|---|---|---|---|---|---|---|---|
| **1** | benzaldehyde | H | H | H | 2911 | 19.4 | 6.7 |
| **2** | 3-anisaldehyde | $OCH_3$ | H | H | 625 | 7.30 | 11.7 |
| **3** | 4-anisaldehyde | H | $OCH_3$ | H | 856 | 4.63 | 5.4 |
| **4** | 3-tolualdehyde | $CH_3$ | H | H | 686 | 6.22 | 9.1 |
| **5** | 4-tolualdehyde | H | $CH_3$ | H | 1545 | 3.69 | 2.4 |
| **6** | 3-fluorobenzaldehyde | F | H | H | 2293 | 27.6 | 12.0 |
| **7** | 4-fluorobenzaldehyde | H | F | H | 4843 | 33.4 | 6.9 |
| **8** | 3,4-difluorobenzaldehyde | F | F | H | 4291 | 24.1 | 5.6 |
| **9** | 3-chlorobenzaldehyde | Cl | H | H | 968 | 20.3 | 21.0 |
| **10** | 4-chlorobenzaldehyde | H | Cl | H | 1409 | 12.5 | 8.9 |
| **11** | 3,4-dichlorobenzaldehyde | Cl | Cl | H | 744 | 13.4 | 18.0 |
| **12** | 3,5-dichlorobenzaldehyde | Cl | H | Cl | 442 | 6.13 | 13.9 |
| **13** | 3-bromobenzaldehyde | Br | H | H | 518 | 12.1 | 23.4 |
| **14** | 4-bromobenzaldehyde | H | Br | H | 967 | 8.60 | 8.9 |
| **15** | 3-cyanobenzaldehyde | CN | H | H | 855 | 12.8 | 15.0 |
| **16** | 4-cyanobenzaldehyde | H | CN | H | 782 | 10.8 | 13.8 |
| **17** | 3-nitrobenzaldehyde | $NO_2$ | H | H | 765 | 12.6 | 16.5 |
| **18** | 4-nitrobenzaldehyde | H | $NO_2$ | H | 461 | 9.47 | 20.5 |
| **19** | 3-(benzyloxy)benzaldehyde | $OCH_2C_6H_5$ | H | H | 360 | 13.2 | 36.7 |
| **20** | 4-(benzyloxy)benzaldehyde | H | $OCH_2C_6H_5$ | H | 218 | 6.35 | 29.1 |
| **21** | 3-phenoxybenzaldehyde | $OC_6H_5$ | H | H | 158 | 26.1 | 165 |
| **22** | 4-phenoxybenzaldehyde | H | $OC_6H_5$ | H | 85 | 5.27 | 62.0 |
| **23** | 3-(4-methylphenoxy)benzaldehyde | (4-$CH_3$-$C_6H_4$)O | H | H | 243 | 23.4 | 96.3 |
| **24** | 3-(4-chlorophenoxy)benzaldehyde | (4-Cl-$C_6H_4$)O | H | H | 164 | 24.1 | 147 |
| **25** | 3-(3,4-dichlorophenoxy)benzaldehyde | (3,4-diCl-$C_6H_3$)O | H | H | 212 | 24.5 | 116 |
| **26** | 3-(3,5-dichlorophenoxy)benzaldehyde | (3,5-diCl-$C_6H_3$)O | H | H | 385 | 5.09 | 13.2 |
| **27** | 4-biphenylcarboxaldehyde | H | $C_6H_5$ | H | 369 | 4.52 | 12.3 |

[a] Kinetic parameters were obtained from Hanes−Woolf plots ($S/V$ vs $S$) with at least six substrate concentrations, each tested in duplicate.

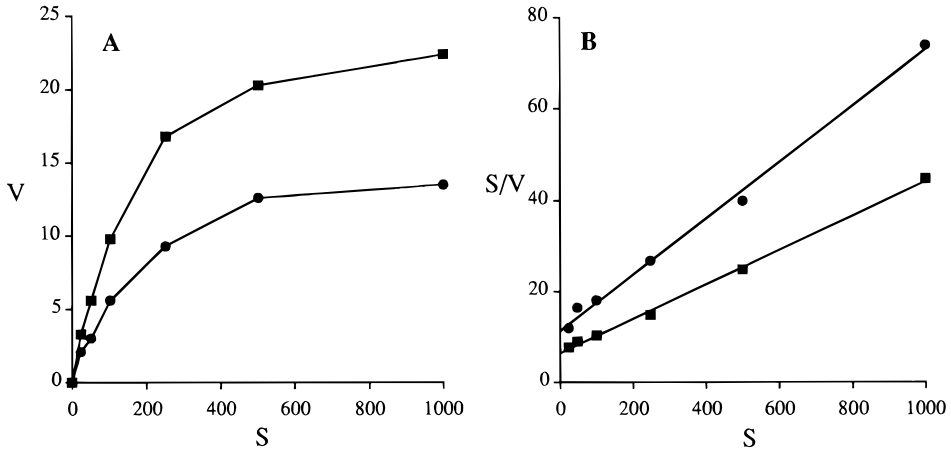


**Figure 2.** Kinetic analysis of the dehydrogenation of 3-phenoxybenzaldehyde (■) and butanal (●) by the purified mALDH: (A) direct plot of reaction velocity ($V$) as a function of substrate concentration ($S$); (B) Hanes−Woolf plot of ($S/V$) as a function of $S$. Units: $V$, nmol of NADH produced min$^{-1}$ ($\mu$g of protein)$^{-1}$ and $S$, $\mu$M.

comparable with those determined for the optimal aliphatic substrates. Figure 2 compares the kinetic properties of 3-phenoxybenzaldehyde and butanal. It is noteworthy that the presence of substituents on the 3-phenoxy group did not influence the efficiency of enzymic dehydrogenation, except in the case of the 3′,5′-dichloro compound (**26**). This substrate exhibited a 2.4-fold larger $K_m$ and a 5-fold lower $V_{max}$ than the unsubstituted analogue (Table 3). Inclusion of highly hydrophilic (hydroxy and carboxy) or extremely bulky (3,4-dibenzyloxy) groups resulted in derivatives that did not undergo detectable dehydrogenation (data not shown).

Several ($\omega$-phenylalkyl)aldehydes were evaluated as substrates of the mALDH. From the data in Table 4 it is apparent that inclusion of one and two methylene groups (**28** and **29**, respectively) between the phenyl ring and carbonyl system resulted in a marked increase in substrate affinity (as reflected by $K_m$ values) and efficiency ($V_{max}/K_m$). Substitution of the phenyl ring of **28** with chlorine atoms at the 3- and 4-positions resulted in relatively poor substrates (Table 4). The isomeric (chlorophenyl)acetaldehydes were slightly inferior to the corresponding chlorobenzaldehydes (**9**, **10**). Thus, it is noteworthy that the substrate preference of the mALDH

**Table 4. Kinetic Parameters of the Dehydrogenation of Arylalkylaldehydes by the mALDH[a]**

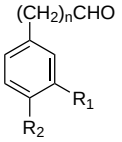


| | aldehyde | $R_1$ | $R_2$ | $n$ | $K_m$ ($\mu$M) | $V_{max}$ nmol min$^{-1}$ ($\mu$g of protein)$^{-1}$ | $10^6 V_{max}/K_m$ |
|---|---|---|---|---|---|---|---|
| **1** | benzaldehyde | H | H | 0 | 2910 | 19.4 | 6.7 |
| **28** | phenylacetaldehyde | H | H | 1 | 180 | 18.5 | 103 |
| **29** | dihydrocinnamaldehyde | H | H | 2 | 51 | 15.4 | 302 |
| **30** | (3-chlorophenyl)acetaldehyde | Cl | H | 1 | 1190 | 11.6 | 9.7 |
| **31** | (4-chlorophenyl)acetaldehyde | H | Cl | 1 | 3380 | 7.75 | 2.3 |

[a] Kinetic parameters were obtained from Hanes−Woolf plots ($S/V$ vs $S$) with at least six substrate concentrations, each tested in duplicate.

**Table 5. Regression Analysis of the Michaelis Constants of Substituted Benzaldehydes as Substrates for the mALDH**

| eq no.[a] | | intercept | $r$ | $s$ | $F$ | $P$ | PRESS | $Q^2$ | $s_{PRESS}$ |
|---|---|---|---|---|---|---|---|---|---|
| | All Compounds Included in Analysis | | | | | | | | |
| 1 | $0.337^1\chi$ (0.043)[b] | 1.985 | 0.84 | 0.24 | 62 | <0.001 | 1.42 | 0.69 | 0.24 |
| 2 | $0.301^0\chi_4 + 0.345^2\kappa_3$ (0.042) (0.045) | 2.592 | 0.86 | 0.23 | 35 | <0.001 | 1.25 | 0.72 | 0.23 |
| 3 | $0.148^1\kappa_4 + 0.260^3\kappa_3 + 0.115^0\chi$ (0.048) (0.107) (0.035) | 2.084 | 0.89 | 0.21 | 29 | <0.001 | 1.02 | 0.77 | 0.21 |
| 4 | $0.142^0\kappa_4 + 0.207^3\kappa_3 + 0.414\sigma_4 + 0.121^0\chi$ (0.041) (0.085) (0.189) (0.032) | 2.131 | 0.90 | 0.20 | 24 | <0.001 | 0.90 | 0.80 | 0.20 |
| | Only 3-Substituted Analogues Included in Analysis | | | | | | | | |
| 5 | $0.163^0\chi$ (0.024) | 2.123 | 0.87 | 0.21 | 45 | <0.001 | 0.68 | 0.75 | 0.21 |
| 6 | $1.590^3\chi_C - 0.153\Xi$ (0.330) (0.046) | 3.012 | 0.85 | 0.24 | 17 | <0.01 | 0.79 | 0.71 | 0.24 |
| 7 | $2.396^3\chi_C - 0.247\Xi - 0.939^4\chi_{PC_3}$ (0.445) (0.056) (0.397) | 3.061 | 0.90 | 0.21 | 17 | <0.001 | 0.55 | 0.80 | 0.20 |
| | Only 4-Substituted Analogues Included in Analysis | | | | | | | | |
| 8 | $0.314^0\chi_4$ (0.044) | 2.580 | 0.91 | 0.22 | 51 | <0.001 | 0.54 | 0.82 | 0.22 |
| 9 | $0.350^0\chi_4 + 0.444\sigma_4$ (0.037) (0.160) | 2.479 | 0.95 | 0.17 | 45 | <0.001 | 0.30 | 0.90 | 0.17 |
| 10 | $0.248^1\kappa_4 + 1.099^3\chi_C$ (0.036) (0.483) | 2.290 | 0.93 | 0.20 | 31 | <0.001 | 0.32 | 0.86 | 0.20 |

[a] $r$, correlation coefficient; $s$, standard deviation of the regression; $F$, $F$ ratio; $P$, level of significance of regression; PRESS, predictive residual sum of squares; $Q^2$, squared correlation coefficient of predictions; $s_{PRESS}$, standard deviation of predictions. [b] Values in parentheses are standard deviations of the parameter coefficients.

for the 3-isomer over the 4-isomer was observed for the benzaldehydes and phenylacetaldehydes.

Immunoinhibition experiments were undertaken in hepatic microsomes using an IgG fraction raised in rabbits against the homogeneous rat mALDH. Preincubation of this IgG fraction with hepatic microsomes (ratio 1−10 mg of IgG/mg of microsomal protein) produced similar extents of inhibition in the rates of dehydrogenation of 3-phenoxybenzaldehyde and decanal (Figure 3). Thus, less than 20% of the microsomal activity remained in fractions that had been preincubated with 10 mg of anti-mALDH IgG/mg of microsomal protein for 30 min prior to determination of substrate dehydrogenation. This experiment confirmed the involvement of the mALDH in the dehydrogenation of aromatic aldehydes, such as 3-phenoxybenzaldehyde, in the microsomal environment.

**QSAR Analysis of the Dehydrogenation of Aromatic Aldehydes by the Rat Hepatic mALDH.** A QSAR was developed for the dehydrogenation of 27 aromatic aldehydes that were mono- or disubstituted at the 3-/4-positions. From Table 5 it is apparent that up to 81% of the data variance in the logarithm (base 10) of the $K_m$ values of the compounds was explained by eq 4. This equation suggests that the capacity of the mALDH

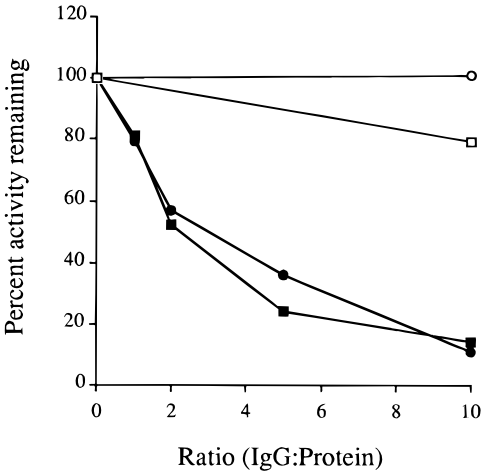


**Figure 3.** Immunoinhibition of microsomal decanal (●) and 3-phenoxybenzaldehyde (■) dehydrogenation activities in adult male rat liver by an IgG preparation raised against the purified mALDH. Open symbols indicate the effect of preimmune IgG on the activities. Microsomal protein (40 $\mu$g), substrate (25 $\mu$M), and varying quantities of IgG (1:1−10:1) were preincubated at 37 °C for 30 min prior to initiation of the reaction with NAD (1 mM). Data are means of duplicate determinations.

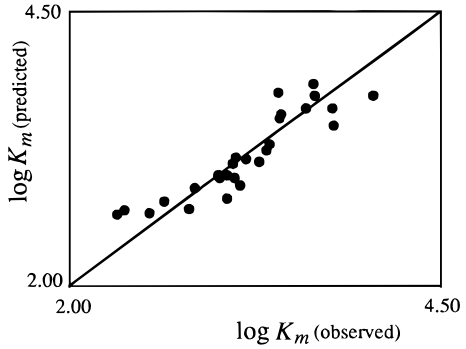


**Figure 4.** Relationship between observed and predicted $K_m$ values for aromatic aldehydes as substrates of the homogeneous mALDH. Predicted values were obtained with eq 4. The diagonal line indicates the relationship log $K_m$(observed) = log $K_m$(predicted). Units: $K_m$, M.

to accommodate aromatic aldehydes is related to the shape of the 3- and 4-substituents, the electronic character of the 4-substituent, and the zero-order connectivity function described by the entire molecule. All parameters in this equation have positive coefficients so that increasing the number of constituent atoms in these substrates and the shape properties of the 3- and 4-substituents contributes directly to affinity. The presence of electron-withdrawing substituents also promotes dehydrogenation. It should be added that optimal atom numbers and shape properties may exist in these substrates, but the present data set did not enable this assertion to be evaluated. Figure 4 presents the relationship between log $K_m$ values that were determined experimentally and calculated using eq 4. The direct relationship between observed and predicted values is indicated by the diagonal line. Thus it can be seen that, although log $K_m$ values of several substrates were under- or overpredicted, these deviations were not excessive.

Table 5 also contains the best regression equations that contained fewer variables. From this analysis it is evident that connectivity and shape parameters (determined over a range of path lengths) appear to be generally important. When the 3- or 4-substituted derivatives were subjected separately to correlation analysis, similar findings were obtained. Equation 7 successfully accounted for 81% of the data variance in the apparent affinity of the dehydrogenase for 3-substituted compounds in terms of steric and three-path cluster connectivity functions derived from the entire molecule and a branched four-path function derived from the 3-substituent. In contrast, correlation of log $K_m$ with connectivity and electronic parameters derived from the 4-substituent yielded eq 9, which enabled explanation of 90% of the data variance. Table 6 illustrates for several of the major equations (eqs 3, 4, 7, 9, 10), that the parameters employed were not significantly collinear ($r^2 \leq 0.423$).

**Table 6. Squared Correlation Matrices ($r^2$) for Collinearity among Variables**

All Compounds; Equation 3

| | $^1\kappa_4$ | $^3\kappa_3$ | $^0\chi$ |
|---|---|---|---|
| $^1\kappa_4$ | 1.000 | 0.394 | 0.018 |
| $^3\kappa_3$ | | 1.000 | 0.275 |
| $^0\chi$ | | | 1.000 |

Equation 4

| | $^0\kappa_4$ | $^3\kappa_3$ | $\sigma_4$ | $^0\chi$ |
|---|---|---|---|---|
| $^0\kappa_4$ | 1.000 | 0.172 | 0.078 | 0.089 |
| $^3\kappa_3$ | | 1.000 | 0.030 | 0.275 |
| $\sigma_4$ | | | 1.000 | 0.060 |
| $^0\chi$ | | | | 1.000 |

3-Substituted Analogues only; Equation 7

| | $^3\chi_C$ | $\Xi$ | $^4\chi_{PC_3}$ |
|---|---|---|---|
| $^3\chi_C$ | 1.000 | 0.000 | 0.423 |
| $\Xi$ | | 1.000 | 0.298 |
| $^4\chi_{PC_3}$ | | | 1.000 |

4-Substituted Analogues only; Equation 9

| | $^0\chi_4$ | $\sigma_4$ |
|---|---|---|
| $^0\chi_4$ | 1.000 | 0.125 |
| $\sigma_4$ | | 1.000 |

Equation 10

| | $^1\kappa_4$ | $^3\chi_C$ |
|---|---|---|
| $^1\kappa_4$ | 1.000 | 0.054 |
| $^3\chi_C$ | | 1.000 |

## Discussion

Aliphatic aldehydes, especially hexanal and longer alkyl chains, are known to be high-affinity substrates for the mALDH ($K_m$'s of 15 $\mu$M and lower) (*11*−*13*). In the present study, decanal appeared to be the optimal substrate but similar $K_m$ and $V_{max}$ values were obtained with the $C_9$−$C_{12}$ analogues. Branched aliphatic aldehydes were also substrates of the mALDH. Methyl substitution at the α-carbon reduced the dehydrogenation rate with respect to the *n* isomer, and substitution at the carbon $\beta$ to the carbonyl group led to a decrease in the affinity of the aldehyde for the enzyme. Because the hydrophobic character of the branched-chain aldehydes would be expected to differ only slightly from the corresponding *n*-alkyl isomers, it appears likely that hydrophobicity is not the sole factor that determines the capacity of the mALDH to support dehydrogenation of these substrates. In the case of the mALDH, it is quite reasonable that hydrophobicity should be an important determinant of substrate specificity. That this enzyme is situated in the hepatic endoplasmic reticulum would favor substrates that are able to partition efficiently into the microsomal membrane. However, by this reasoning, aromatic aldehydes should also be substrates of the enzyme.

From pre-steady-state and burst kinetics, the rate-limiting step for ALDH was suggested to occur after formation of the thioacyl intermediate (*29*). This is depicted in Scheme 1 as steps 2−4. In the case of the horse liver mitochondrial enzyme, deacylation (step 4) is considered to be the rate-determining step (*5*, *29*), whereas cofactor dissociation (step 5) has been proposed in the case of the human hepatic cytosolic enzyme (*30*). Delocalization of the electron density from the carbonyl functionality to the aromatic system would occur in the present series of substituted benzaldehydes. By comparison, the alkyl substituents in aliphatic aldehydes would tend to push electrons into the carbonyl group. These electronic effects would influence the potential

**Scheme 1. Reaction Mechanism of mALDH[a]**

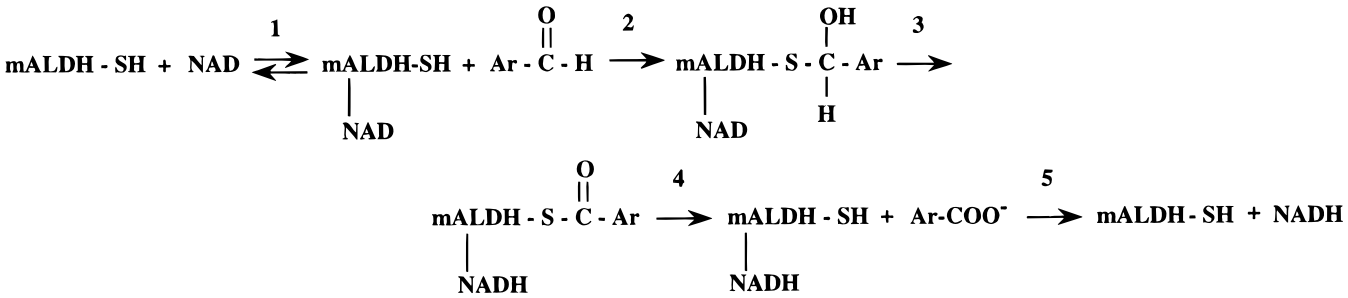


[a] SH refers to the catalytic cysteine residue, NAD/NADH are the oxidized/reduced forms of the cofactor, and ArCHO is an aromatic aldehyde. Step 1 shows the binding of oxidized cofactor to the enzyme, step 2 is the nucleophilic attack of the mALDH cysteine at the aldehyde carbonyl to generate a thiohemiacetal, step 3 shows the rearrangement of the intermediate with hydride transfer to NAD, step 4 depicts hydrolysis of the thioester intermediate with liberation of carboxylate and cofactor-bound mALDH, and step 5 shows dissociation of the reduced cofactor from the enzyme.

energy required for hydride removal from the enzyme−substrate transition state, and it is uncertain whether the rate-limiting step would be common to the dehydrogenation of both aliphatic and aromatic aldehydes.

Compared with benzaldehyde, the arylalkylaldehydes phenylacetaldehyde and dihydrocinnamaldehyde were dehydrogenated effectively. This finding is in accord with the observation that aliphatic aldehydes are superior to their aromatic counterparts as substrates for the mALDH. Substitution of phenylacetaldehyde with a chlorine atom in the 3- or 4-position of the aromatic system produced substrates that were dehydrogenated much less efficiently than the parent. It is evident from the $V_{max}/K_m$ ratios in Tables 3 and 4 that 3-chlorobenzaldehyde and (3-chlorophenyl)acetaldehyde underwent dehydrogenation with 2.4- and 4.2-fold greater efficiency than their respective 4-isomers.

Evidence in the literature suggests that hydrophobic properties may not be the only factors that influence the interaction of aldehydes with the mALDH. *Ortho*-substituted halobenzaldehydes were found not to undergo microsomal dehydrogenation to the corresponding acids, whereas certain 3- and 4-substituted aldehydes were dehydrogenated at measurable rates (*14*). This was confirmed in the present study from which it appears likely that the detrimental effect of the *ortho* substituent is steric and not electronic in nature.

3-Substituted aromatic aldehydes were usually better substrates than 4-substituted compounds for the mALDH. Despite this generalization, 4-phenoxybenzaldehyde (**22**) was found to have the highest affinity (lowest $K_m$) for the mALDH; however, its $V_{max}$ was quite small. The 3-phenoxybenzaldehydes (**21**, **23**−**25**) were found to be the next most efficient substrates. 3-Phenoxybenzaldehyde itself was ~20-fold more efficient ($V_{max}/K_m$) than benzaldehyde as a substrate for mALDH but, compared with the aliphatic aldehydes, was only about as efficient as pentanal and was 50-fold less efficient than decanal. Since it was also noted that 3-phenoxybenzaldehyde was the most efficient substituted aromatic substrate, a number of other 3-phenoxybenzaldehydes (**23**−**26**) were evaluated as substrates. It appeared that substitution of the 3-phenoxy system at either the 3′- or 4′-positions had only a relatively minor effect on the efficiency of the reaction, but the 3′,5′-dichloro-substituted analogue (**26**) was a poor substrate. Shape and steric factors may be responsible for this effect. Perhaps 3′,5′-disubstitution prevents the rotation of the substituent so as to minimize an adverse steric interaction within the active center of the enzyme (Figure 5). This should be viewed with caution,

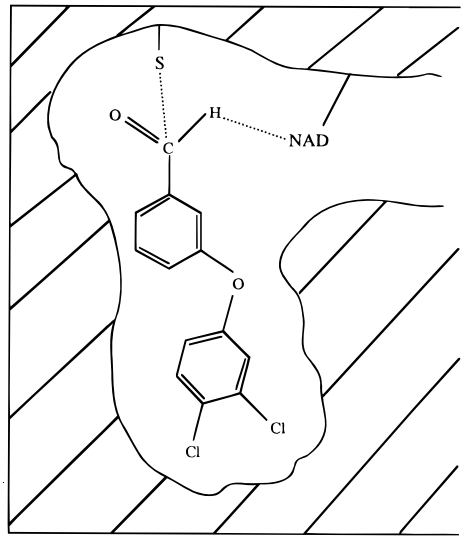


**Figure 5.** Possible orientation of aromatic aldehydes within the active center of the mALDH. Features include the catalytic cysteine (indicated by the sulfur atom coordinated with the carbonyl group), the NAD molecule bound at the adjacent cofactor site and interacting with the carbonyl hydrogen atom, and the narrow cleft that is able to accommodate certain 3- and 4-substituted, but not 2-substituted, aromatic aldehydes.

however, because it was not possible to describe adequately the electronic effects of phenoxy substitution at the carbonyl function within this set of substituted 3-phenoxybenzaldehydes.

The optimal QSAR equation identified several parameters as important contributors to substrate affinity, including the zero-order connectivity function of the whole molecule ($^0\chi$), the shapes of the 3- and 4-substituents ($\kappa$), and the electronic nature of the 4-substituent ($\sigma$). Similar parameters appeared to contribute strongly to regression equations when 3- or 4-substituted aromatic aldehydes were considered as separate subgroups. The zero-order molecular connectivity function ($^0\chi$) considers only the arrangement of atoms within a structure. Although the physical interpretation of these parameters is not completely clear, their relatedness to molecular properties like polarizability, partition coefficient, and surface area has been demonstrated (*31*). Indeed, the spatial arrangement of atoms within a structure is a fundamental property, probably more so than, for example, partitioning between immiscible phases, which is commonly taken to represent hydrophobic effects.

Van der Waals interactions, including polarizability (Keesom and Debye forces) and dispersion (London)

forces, relate to perturbations in the distribution of electrons between atoms. In contrast, hydrophobic interactions have been largely explained in terms of London forces, which are the weakest of the three types of van der Waals interactions. Because the present study described the correlation of log $K_m$ with $^0\chi$ rather than with hydrophobic character (e.g., log *P*), it is likely that substrate behavior is dependent upon van der Waals interactions other than London forces.

Effective molecular volume is greater where there is hydrogen bonding to substituent groups. Koehler *et al.*, have defined the isotropic surface, which is essentially the surface area of the nonpolar region of a molecule that is accessible to nonspecific interactions (*32*). Hydrophilic regions, such as hydroxyl or carboxyl substituents with their associated waters of solvation, are excluded from the calculation of the isotropic surface. Thus, interaction of an enzyme and substrate would be a balance between favorable (attractive) van der Waals interactions, between amino acid residues at the active center and the isotropic surface of the molecule, and unfavorable (repulsive) interactions due to steric and electronic factors. In the case of the mALDH, the presence of hydrophilic substituents in the 3- or 4-positions of benzaldehyde may sterically hinder the appropriate orientation of the substrate at the active center. Similarly the low activity of benzaldehydes possessing large substituents in both the 3- and 4-positions may be due to steric hindrance. In such cases, unfavorable interactions outweigh favorable ones.

The possible orientation of 3-phenoxybenzaldehyde in the active site of the mALDH is shown in Figure 5. The approximate dimensions of this molecule would be 7.5 Å by 12 Å, including the van der Waals radii, and the aromatic system itself, including the $\pi$ orbitals, is between 5 and 6 Å deep. This structure and the observed rates of substrate dehydrogenation could be accommodated if the active site of the mALDH contains a relatively narrow cleft (as depicted in Figure 5). This model also accounts for the unfavorable effect of *ortho* substitution on substrate behavior. Adverse steric interactions between an *ortho* substituent and either the cofactor (NAD, bound at the adjacent cofactor site) or the substrate cleft itself are probably responsible for the undetectable rates of dehydrogenation of these substrates.

The model of the mALDH active site in Figure 5 takes into account the apparent importance of the shapes of the 3- and 4-substituents as determinants of $K_m$. The zero-order shape attribute of the 4-substituent in the aromatic aldehydes ($^0\kappa_4$) has been likened to the property of symmetry, whereas the third-order shape attribute of the 3-substituent ($^3\kappa_3$) is believed to encode a feature of central branching (*24*). The final parameter that appeared in the best regression equation was the Hammett constant of the 4-substituent ($\sigma_4$). Aldehydes containing electron-donating groups, such as methyl and methoxy, were substrates inferior to benzaldehyde. Strongly electron-withdrawing groups in the 4-position, such as nitro and cyano, promoted dehydrogenation. The complex nature of the 3-substituent in several of the substrates led to problems in the detailed assessment of any electronic effect at this position. However, the electronic effects of substituents of the phenoxy system should be insignificant at the benzaldehyde carbonyl group.

The catalytic mechanism of the mitochondrial ALDH is depicted in Scheme 1 and appears to involve the initial nucleophilic attack of the Cys-302 sulfur at the carbonyl carbon of the substrate to form a thiohemiacetal, followed by hydride transfer from the substrate to NAD and the formation of a thioester intermediate (*5*). Although yet to be demonstrated directly for each ALDH, sequence alignments suggest that Cys-241 is probably the corresponding residue in the mALDH (*5, 10*). Hydrolysis of the thioester releases the carboxylic acid product and regenerates the enzyme, which can accept further substrate molecules. The presence of electron-withdrawing substituents ($\sigma$ positive) would be expected to favor dehydrogenation by enhancing the partial positive character of the carbonyl carbon. This was noted in the present study as well as in another study of benzaldehydes containing simple substituents as substrates for a bacterial ALDH (*33*).

The functional role of the mALDH has yet to be completely clarified. It has been suggested that the enzyme may detoxify aldehydic products of microsomal lipid peroxidation (*12*). Such toxic aldehydes, including alkanals, alkenals, ketones, and hydroxyalkenals, are generated *in vitro* during lipid peroxidation in carbon tetrachloride- or iron-ADP-containing systems (*34*). It is feasible that the enzyme may function in the elimination of alkanals and alkenals since the quantities of these agents that are formed during lipid peroxidation would be adequate for saturation of the mALDH ($> K_m$). From the present analysis, ALDHs may also have a role in the dehydrogenation of xenobiotic aromatic aldehydes, and those formed *in vivo* from oxidation of neurotransmitters, to the corresponding aryloxybenzoic acids.

**Acknowledgment.** This study was supported by a grant from the Australian National Health and Medical Research Council. R.M. was the recipient of an Astra/Gastroenterological Society of Australia Career Development Award.

## References

(1) Lindahl, R. (1992) Aldehyde dehydrogenases and their role in carcinogenesis. *Crit. Rev. Biochem. Mol. Biol.* **27**, 283−335.
(2) Lindahl, R., and Evces, S. (1984) Rat liver aldehyde dehydrogenase. I. Isolation and characterization of four high $K_m$ normal liver isozymes. *J. Biol. Chem.* **259**, 11986−11990.
(3) Lindahl, R., and Evces, S. (1984) Rat liver aldehyde dehydrogenase. II. Isolation and characterization of four inducible isozymes. *J. Biol. Chem.* **259**, 11991−11996.
(4) Senior, D. J., and Tsai, C. S. (1988) Purification and characterization of aldehyde dehydrogenase from rat liver mitochondria. *Arch. Biochem. Biophys.* **262**, 211−220.
(5) Farres, J., Wang, T. T. Y., Cunningham, S. J., and Weiner, H. (1995) Investigation of the active site cysteine residue of rat liver mitochondrial aldehyde dehydrogenase by site-directed mutagenesis. *Biochemistry* **34**, 2592−2598.
(6) Dunn, T. J., Koleske, A. J., Lindahl, R., and Pitot, H. C. (1989) Phenobarbital-inducible aldehyde dehydrogenase in the rat. cDNA sequence and regulation of the mRNA by phenobarbital in responsive rats. *J. Biol. Chem.* **264**, 13057−13065.
(7) Evces, S., and Lindahl, R. (1989) Characterization of rat cornea aldehyde dehydrogenase. *Arch. Biochem. Biophys.* **274**, 518−524.
(8) Dunn, T. J., Lindahl, R., and Pitot, H. C. (1988) Differential gene expression in response to 2,3,7,8-tetrachlorodibenzo-*p*-dioxin (TCDD). Noncoordinate regulation of a TCDD-induced aldehyde dehydrogenase and cytochrome P-450c in the rat. *J. Biol. Chem.* **263**, 10878−10886.
(9) Jones, D. E., Brennan, M. D., Hempel, J., and Lindahl, R. (1988) Cloning and complete nucleotide sequence of a full-length cDNA encoding a catalytically functional tumor-associated aldehyde dehydrogenase. *Proc. Natl. Acad. Sci. U.S.A.* **85**, 1782−1786.
(10) Miyauchi, K., Masaki, R., Taketani, S., Yamamoto, A., Akayama, M., and Tashiro, Y. (1991) Molecular cloning, sequencing, and expression of cDNA for rat liver microsomal aldehyde dehydrogenase. *J. Biol. Chem.* **266**, 19536−19542.

(11) Mitchell, D. Y., and Petersen, D. R. (1989) Oxidation of aldehydic products of lipid peroxidation by rat liver microsomal aldehyde dehydrogenase. *Arch. Biochem. Biophys.* **269**, 11−17.
(12) Lindahl, R., and Petersen, D. R. (1991) Lipid aldehyde oxidation as a physiological role for class 3 aldehyde dehydrogenases. *Biochem. Pharmacol.* **41**, 1583−1587.
(13) Antonenkov, V. D., Pirozhkov, S. V., and Panchenko, L. F. (1987) On the role of microsomal aldehyde dehydrogenase in metabolism of aldehydic products of lipid peroxidation. *FEBS Lett.* **224**, 357−360.
(14) Rietveld, E. C., de Zwart, M., Cox, P. G. F., and Seutter-Berlage, F. (1987) Substituent effects during the rat liver aldehyde dehydrogenase catalyzed oxidation of aromatic aldehydes. *Biochim. Biophys. Acta* **914**, 162−169.
(15) Karabatsos, G. J., and Bushman, D. W. (1975) Structural studies by nuclear magnetic resonance. XXIII. Conformational analysis of substituted phenylacetaldehydes. *Tetrahedron* **31,** 1471−1475.
(16) Murray, M., Wilkinson, C. F., and Dube, C. E. (1983) Effects of dihydrosafrole on cytochrome P-450 and drug oxidation in hepatic microsomes from control and induced rats. *Toxicol. Appl. Pharmacol.* **68**, 66−76.
(17) Lowry, O. H., Rosebrough, N. J., Farr, A. L., and Randall, R. J. (1951) Protein measurement with the Folin phenol reagent. *J. Biol. Chem.* **193,** 265−275.
(18) Nakayasu, H., Mihara, K., and Sato, R. (1978) Purification and properties of a membrane-bound aldehyde dehydrogenase from rat liver microsomes. *Biochem. Biophys. Res. Commun.* **83**, 697−703.
(19) Laemmli, U. K. (1970) Cleavage of structural proteins during assembly of the head of bacteriophage T4. *Nature* **227**, 680−685.
(20) Hansch, C., Leo, A., Unger, S. H., Kim, K. H., Nikaitani, D., and Lien, E. J. (1973) Aromatic substituent constants for structure−activity correlations. *J. Med. Chem.* **16**, 1207−1216.
(21) Hansch, C., Rockwell, S. D., Jow, P. Y. C., Leo, A., and Steller, E. E. (1977) Substituent constants for correlation analysis. *J. Med. Chem.* **20**, 304−306.
(22) Kier, L. B., and Hall, L. H. (1976) *Molecular Connectivity in Chemistry and Drug Design*, Academic Press, New York.
(23) Kier, L. B. (1980) Molecular connectivity as a descriptor of structure for SAR analyses. In *Physical Chemical Properties of Drugs* (Yalkowsky, S. H., Sinkula, A. A., and Valvani, S. C., Eds.) pp 277−319, Marcel Dekker, New York.
(24) Kier, L. B. (1987) Indexes of molecular shape from chemical graphs. *Med. Res. Rev.* **7**, 417−440.
(25) Kier, L. B. (1987) A substituent steric effect index based on the molecular graph. *Quant. Struct.-Act. Relat.* **6**, 117−122.
(26) Cramer, R. D., III, Bunce, J. D., Patterson, D. E., and Frank, I. E. (1988) Crossvalidation, bootstrapping, and partial least squares compared with multiple regression in conventional QSAR studies. *Quant. Struct.-Act. Relat.* **7**, 18−25.
(27) Kim, K. H. (1992) 3D-Quantitative structure-activity relationships: Investigation of steric effects with descriptors directly from 3D structures using a comparative molecular field analysis (CoMFA) approach. *Quant. Struct.-Act. Relat.* **11**, 453−460.
(28) Kubinyi, H. (1994) Variable selection in QSAR studies. I. An evolutionary algorithm. *Quant. Struct.-Act. Relat.* **13**, 285−294.
(29) Weiner, H., Hu, J. H. J., and Sanny, C. G. (1976) Rate-limiting steps for the esterase and dehydrogenase reaction catalyzed by horse liver aldehyde dehydrogenase. *J. Biol. Chem.* **251**, 3853−3855.
(30) Vallari, R. C., and Pietruszko, R. (1981) Kinetic mechanism of the human cytosolic aldehyde dehydrogenase E1. *Arch. Biochem. Biophys.* **212**, 9−19.
(31) Kier, L. B., Murray, W. J., and Hall, L. H. (1975) Molecular connectivity. 4. Relationships to biological activities. *J. Med. Chem.* **18**, 1272−1274.
(32) Koehler, M. G., Grigoras, S., and Dunn, W. J., III (1988) The relationship between chemical structure and the logarithm of the partition coefficient. *Quant. Struct.-Act. Relat.* **7**, 150−159.
(33) Shaw, J. P., Schwager, F., and Harayama, S. (1992) Substrate-specificity of benzyl alcohol dehydrogenase and benzaldehyde dehydrogenase encoded by TOL plasmid pWW0. Metabolic and mechanistic implications. *Biochem. J.* **283**, 789−794.
(34) Poli, G., Dianzani, M. U., Cheeseman, K. H., Slater, T. F., Lang, J., and Esterbauer, H. (1985) Separation and characterization of the aldehydic products of lipid peroxidation stimulated by carbon tetrachloride or ADP-iron in isolated hepatocytes and rat liver microsomal suspensions. *Biochem. J.* **227**, 629−638.

TX950106L